CrossMark

RESEARCH

First principle investigations on structural, mechanical, spin polarized electronic and magnetic properties of TmZn and TmCd

Satish Chand[1] · R. P. Singh[2] · A. Govindan[3]

Abstract Structural, mechanical, spin polarized electronic and magnetic properties of TmZn and TmCd intermetallic compounds have been studied using the full-potential linearize augmented plane-wave plus local orbital method. The structural and mechanical properties have been studied in terms of lattice parameter (a_0), bulk modulus (B_0) and its first-order pressure derivative (B_0'), elastic constants (C_{ij}), Young's modulus (Y), shear modulus (G) and Poisson's ratio (v) in equilibrium state which are found to be consistent with available experimental/theoretical values. Spin polarized electronic properties have been investigated in terms of band structure and density of state histograms for spin up and spin down channel. Electronic behavior of TmZn and TmCd shows that studied materials are metallic ferromagnets with high spin polarization in which Tm-f state electrons have dominant character.

Keywords Binary intermetallics · Mechanical properties · Electronic structure · Magnetic properties

Introduction

Binary rare earth intermetallic compounds viz. TmZn and TmCd exhibit regular and systematic changes in the physical properties. Binary rare earth intermetallics offers high ductility and high-temperature mechanical strength due to which they are widely used in automobile and aerospace applications, viz. commercial aircraft turbines, etc. [1–4]. Binary rare earth intermetallics are extensively studied also due to their partially filled 4f shells in rare earth atoms and availability of their single crystals. TmZn and TmCd crystallize in space group Pm3m (number 221). In Pm3m space group (221) cubic crystals, the more electronegative atoms are located at the corners of the unit cell, while the more electropositive atoms are located in the center of the unit cell [5]. The typical crystal unit cell for TmZn and TmCd is shown in Fig. 1. From this figure, it can be seen that Zn (or Cd) sits at the center of the cubic unit cell while the rare earth atoms are at the corners.

Neutron diffraction, temperature dependence of thermoelectric power and magneto-elastic studies has been made on several rare earth intermetallic compounds [6–8]. Recently, some more studies on structural, elastic and electronic behavior have been carried out on many rare earth intermetallics [9–13]. But mechanical, spin polarized electronic and magnetic studies have not been made on TmZn and TmCd. Thus, these compounds have been considered for mechanical, spin polarized electronic and magnetic studies. The knowledge of mechanical, spin polarized electronic and magnetic properties of these compounds will help in further understanding and controlling the material properties which are necessary for promoting the future applications of the compounds.

Computational approach

Density functional calculations have been made to investigate the structural, mechanical, spin polarized electronic and magnetic properties of TmZn and TmCd intermetallic

✉ R. P. Singh
  rishisingh79@gmail.com

1 Department of Physics, Mewar University, Chittorgarh, Rajasthan, India

2 Department of Physics, S. S. V. Degree College (Affiliated to C. C. S. University, Meerut U. P.), Hapur, India

3 Department of Physics, M. M. H. College (C. C. S. University-Meerut), Ghaziabad, India
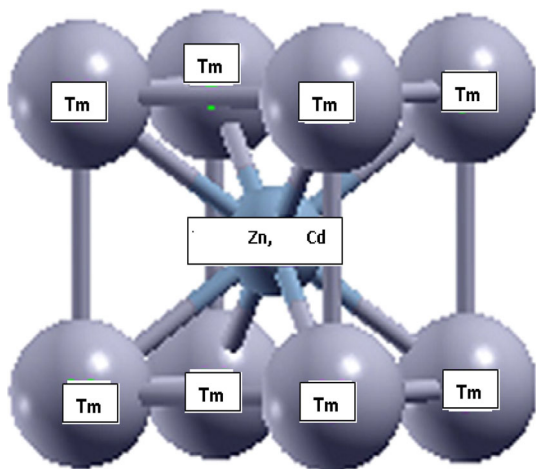
🐾 Springer

Fig. 1 Typical crystal unit cell for TmZn (or TmCd)

compounds. The calculations have been performed using an accurate full-potential linearize augmented plane-wave plus local orbital method (FP-LAPW + lo), implemented in WIEN2k package [14–18]. In this approach, the unit cell is divided into two distinct regions: (i) first region contain all points inside the muffin-tin spheres around the atom (ii) second region is the interstitial region outside the muffin-tin spheres. The potential and the density in the interstitial region are expanded in terms of plane waves while inside the muffin-tin sphere they are expanded in terms of spherical harmonics. Inside the muffin-tin spheres, the expansion of the non-spherical potential and charge density were carried out up to $l_{max} = 10$. The generalized gradient approximation (GGA) has been used to calculate the total energy, which is based on exchange–correlation energy optimization [15]. The k and E convergences were checked by increasing the number of k points and the energy convergences criteria. In the irreducible part of the Brillouin zone, $14 \times 14 \times 14$ k points were used to calculate the total and partial density of states. The lattice parameters were taken to be 3.516 Å for TmZn and 3.665 Å for TmCd [19] for the calculations. The radius of muffin-tin spheres was chosen to be 2.5 a.u. for Tm and 2.4 a.u. for Zn and Cd.

Elastic constants provide the detailed information about mechanical behavior of the materials. The elastic constants and hence other mechanical parameters viz. bulk modulus, shear modulus, Young's modulus, and Poisson's ratio can be determined by calculating the total energy of the crystal system [20, 21]:

Total energy of a crystal in strained state is given by:

$$E_{total} = E_{total}^0 + P(V - V_0) + \phi_{elastic}, \tag{1}$$

where E_{total}^0 is the total energy of unstrained crystal, V_0 is the volume of the crystal in initial state, V is the volume in

strained state, P and $\phi_{elastic}$ are the pressure and elastic energy, respectively, defined by:

$$P = -\left(\frac{\partial E_{total}^0}{\partial V}\right) \tag{2}$$

$$\phi_{elastic} = \frac{V}{2} . C_{ijkl} \varepsilon_{ik} \varepsilon_{jl} \tag{3}$$

Here, $(i, j, k, l = 1, 2, 3)$

In Voigt two suffix notations, $\phi_{elastic}$ is given by:

$$\phi_{elastic} = \frac{V}{2} . C_{ij} \varepsilon_i \varepsilon_j, \tag{4}$$

where C_{ij} are elastic moduli derived from second-order derivative of E_{total} w.r.t. finite strain is given by:

$$C_{ij} = \left(\frac{1}{V_0} \frac{\partial^2 E_{total}}{\partial \varepsilon_i \partial \varepsilon_j}\right)_{\varepsilon=0}. \tag{5}$$

A cubic crystal has only three independent elastic constants, namely, C_{11}, C_{12} and C_{44}. As a result, a set of three equations is needed to determine all the constants. Hence, three types of strain must be applied to the starting crystal.

The first type strain involves calculating the bulk modulus, given by the formula

$$B_0 = (C_{11} + 2C_{12})/3 \tag{6}$$

Second type strain involves performing volume conservative tetragonal strain given by the following tensor:

$$\begin{bmatrix} \varepsilon & 0 & 0 \\ 0 & \varepsilon & 0 \\ 0 & 0 & \dfrac{1}{(1+\varepsilon)^2} - 1 \end{bmatrix}. \tag{7}$$

This strain has an effect on the total energy from its unstrained state given by following equation:

$$E(\varepsilon) = E(0) + 3(C_{11} - C_{12})V_0\varepsilon^2 + o(\varepsilon^3) \tag{8}$$

Finally, for the third type of deformation, we use the volume-conserving rhombohedral strain tensor given by

$$\frac{\varepsilon}{3}\begin{bmatrix} 1 & 1 & 1 \\ 1 & 1 & 1 \\ 1 & 1 & 1 \end{bmatrix} \tag{9}$$

This volume-conserving rhombohedral strain transforms the total energy to

$$E(\varepsilon) = E(0) + \frac{1}{6}(C_{11} + 2C_{12} + 4C_{12})V_0\varepsilon^2 + o(\varepsilon^3). \tag{10}$$

Here, $O(\varepsilon^3)$ indicates that the neglected terms in the polynomial expansion are cubic and higher power of the ε.

Using the three elastic constants C_{11}, C_{12} and C_{44}, other mechanical parameters viz. bulk modulus (B) Young's modulus (Y) isotropic shear modulus (G) and Poisson ratio,

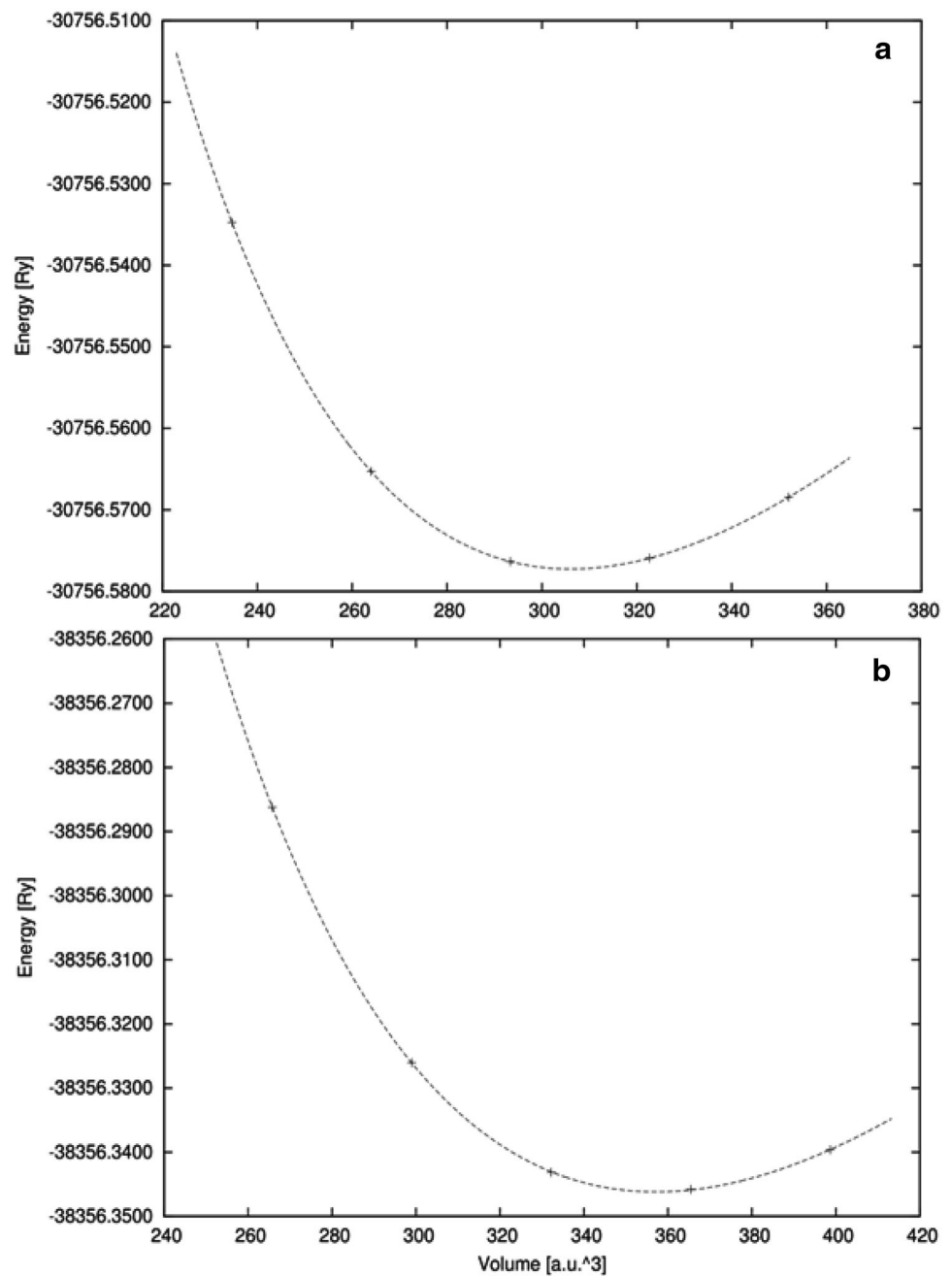**Fig. 2** Total energy as a function of unit cell volume for **a** TmZn **b** TmCd with GGA approximation

Table 1 Lattice constant, a_0 (Å), bulk modulus, B_0 (GPa), pressure derivative of bulk modulus, B_0' (GPa) equilibrium condition (at 0 K) for TmZn and TmCd using GGA

Compounds	a_0	B_0	B_0'
TmZn	3.49	81.23	4.01
Expt.	3.51[a]	–	–
TmCd	3.63	54.33	3.54
Expt.	3.66[a]	–	–

[a] Buschow et al. [19]

(v) can be calculated to show the mechanical behavior using the following explicit expressions:

$$G = (G_V + G_R)/2. \tag{11}$$

Here G_V is Voigt's shear modulus corresponding to the upper bound of G values, and G_R is Reuss's shear modulus for cubic crystals corresponding to the lower bound values, expressed as:

$$G_V = (C_{11} - C_{12} + 2C_{44})/4 \tag{12}$$

$$G_R = 5[(C_{11} - C_{12})C_{44}]/[4C_{44} + 3(C_{11} - C_{12})]. \tag{13}$$

Table 2 Calculated elastic moduli, C_{ij} (GPa), bulk modulus, B (GPa), Young's modulus, Y (GPa), shear modulus, G (GPa) and Poisson ratio, v in equilibrium condition (at 0 K) for TmZn and TmCd using GGA

Compounds	C_{11}	C_{12}	C_{44}	$C_{11}–C_{12}$	B	Y	G	B/G	v	A
TmZn (at 0 K)	117.08	63.37	56.10	53.44	81.45	106.71	41.63	1.95	0.28	2.10
Expt. (at 300 K)	103.03[a,c]	55.23[a,b]	52.20[a,b]	47.80[a,b]	70.70[a,b]	97.00	38.10	1.86	0.27	2.17
TmCd (at 0 K)	99.11	64.42	43.90	33.60	75.65	79.26	29.90	2.52	0.32	2.61
Expt. (at 300 K)	–	–	–	31.37[a]	–	–	–	–	–	–

[a] Wohlfarth et al. [25], [b] Morin et al. [8]

And the expressions for the bulk modulus, Young's modulus and Poisson's ratio are given by:

$$B = \frac{C_{11} + 2C_{12}}{3} \tag{14}$$

$$Y = \frac{9GB}{G + 3B} \tag{15}$$

$$v = (3B - 2G)/(6B + 2G). \tag{16}$$

Elastic anisotropic factor (A) is an important parameter which is the measure of anisotropy of elastic wave velocity in a crystal. For an isotropic material, anisotropic factor (A) is unity and expressed as [22]:

$$A = \frac{2C_{44}}{C_{11} - C_{12}}. \tag{17}$$

Results and discussion

Structural and mechanical properties

The theoretical lattice parameters, bulk modulus and its first-order pressure derivative have been obtained through fitting the total energy data with the Murnaghan equation of state [23, 24] given by:

$$
E_{\text{total}} = E_0(V) \\
+ \frac{B_0 V_0}{B_0'(B_0' - 1)} \left[B_0 \left(1 - \frac{V_0}{V} \right) + \left(\frac{V_0}{V} \right)^{B_0'} - 1 \right], \tag{18}
$$

where $E_0(V)$ and V_0 are the energy and volume at equilibrium. B_0 and B_0' are the equilibrium bulk modulus and its first-order pressure derivative.

The energy versus volume curves (obtained using optimization method) for TmZn and TmCd are shown in Fig. 2a, b. It is clear from these figures that equilibrium volume increases while equilibrium energy decreases from TmZn → TmCd. Its reason is increasing the molecular weight from TmZn → TmCd. Because molecular stability increases with increasing the molecular weight due to which molecules vibrate in the least volume of the unit cell for occupying the equilibrium state. Hence, equilibrium unit cell volume increases and equilibrium energy decreases from TmZn → TmCd.

The calculated lattice parameter (a_0), bulk modulus (B_0) and its first-order pressure derivative (B_0') are shown in Table 1. Calculated values of lattice parameter show good agreement with experimental values [8, 25]. Calculated values of elastic constants (C_{11}, C_{12}, C_{44} and $C_{11}–C_{12}$) are shown in Table 2. To best our knowledge, experimental values of elastic constants for TmZn are given in the
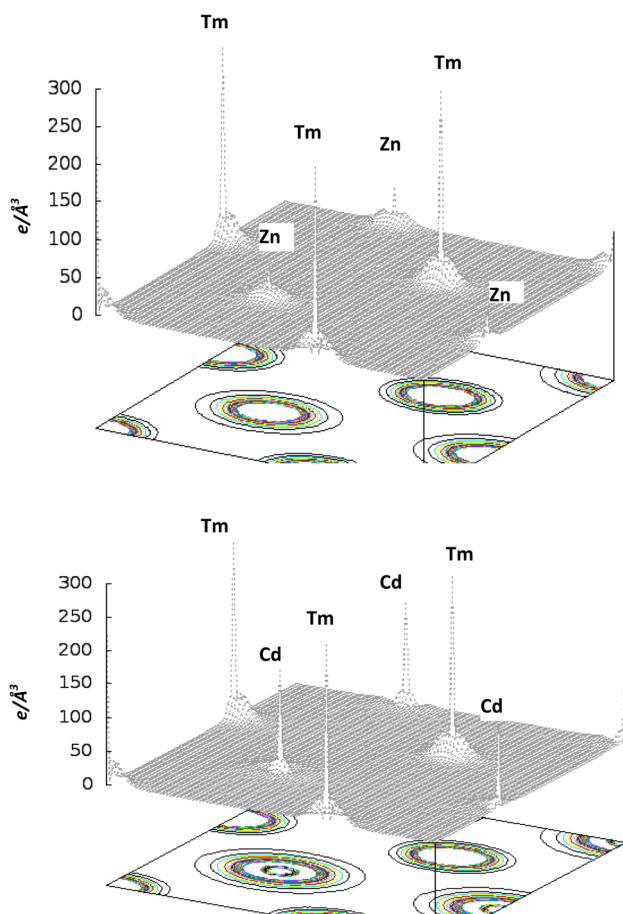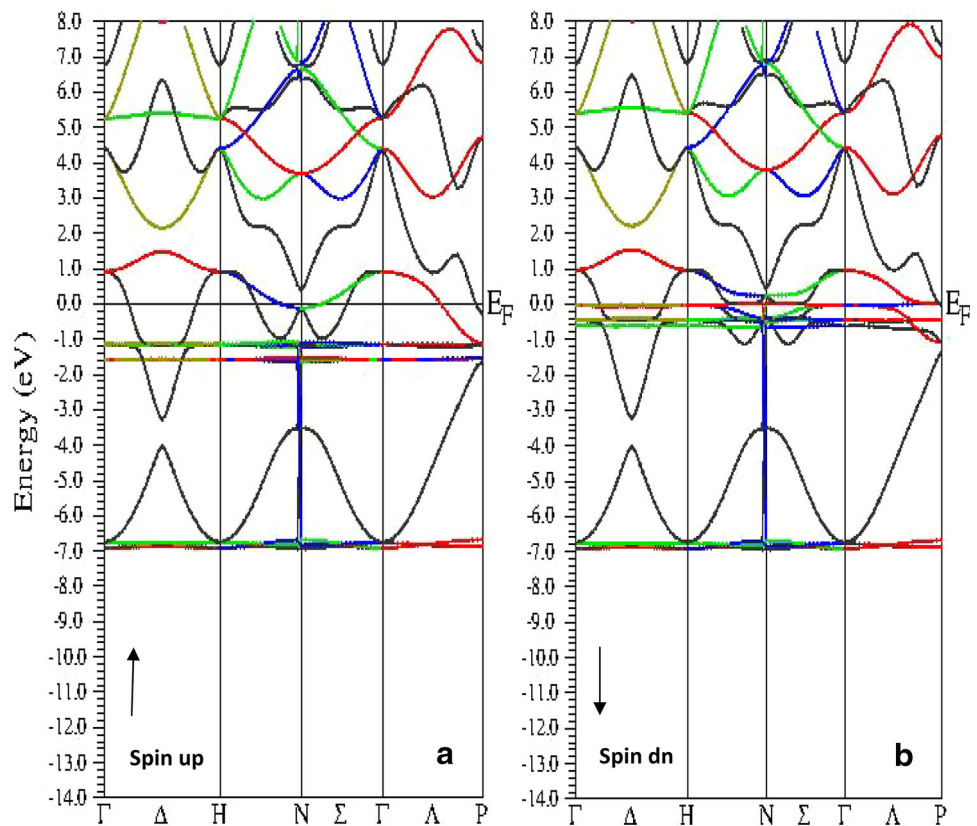

Fig. 3 3d-contour plots of the total valence charge density in (100) plane for **a** TmZn, **b** TmCd

Fig. 4 a Spin polarized
electron dispersion curves along
high symmetry directions in the
Brillouin zone for **a** TmZn_up,
b TmCd_dn

literatures which show good agreement with available experimental values. Our C_{11}, C_{12}, C_{44} and $C_{11}-C_{12}$ values are found to be underestimated by about ≈ 12 %, ≈ 13 %, ≈ 07 % and ≈ 11 %, respectively, for TmZn compared to the experimental value of Wohalfarath et al. [25]. Furthermore, calculated values of elastic constants (C_{ij}) satisfy all mechanical stability conditions ($C_{11}-C_{12} > 0$, $C_{11} > 0$, $C_{44} > 0$, $C_{11} + 2C_{12} > 0$) and cubic stability condition ($C_{12} < B < C_{11}$) [26] that lead to the validity of calculated elastic constants.

The bulk modulus (B) is a material property indicating the degree of resistance of a material to compression. Larger the bulk modulus, greater is the degree of resistance. Shear modulus, G represents the resistance to plastic deformation. The calculated values of B and G are shown in Table 2. It can be observed from Table 2 that $B_{TmZn} > B_{TmCd}$ which indicates that degree of resistance of TmZn is larger than TmCd. The ratio B/G is a parameter which indicates the brittle or ductile behavior of the material proposed by Pugh [27].The critical value of B/G is 1.75. If $B/G > 1.75$, then material indicates ductile behavior. Otherwise, the material behavior is brittle in nature. In our case, B/G value for both the compounds TmZn and TmCd is greater than 1.75 (Table 2). Therefore, both the compounds are ductile and TmCd is found to be more ductile compared to TmZn. Poisson's ratio (υ) also

show ductile/brittle behavior of a material. If $\upsilon > 0.27$, compounds are ductile otherwise brittle in nature. In our case, $\upsilon \approx 0.28$ for TmZn and $\upsilon \approx 0.32$ for TmCd. Therefore, values of υ for TmZn and TmCd also justify that both the compounds are ductile in nature. Furthermore, Poisson's ratio also indicates the compressibility of a material. As $\upsilon \rightarrow 1/2$, material tends to incompressibility [28] and at $\upsilon = 1/2$ the material is nearly incompressible. In our case, value of Poisson's ratio is $\upsilon \approx 0.28$ for TmZn and $\upsilon \approx 0.32$ for TmCd which show that both the compounds are compressible. The stiffness of a material is explained using Young's modulus (Y) [29]. Higher value of Young's modulus indicates larger stiffness. In our case, $Y_{TmZn} > Y_{TmCd}$, indicating TmZn is stiffer than TmCd. Another important parameter is elastic anisotropic factor (A) which is the measure of anisotropy of elastic wave in a crystal. For an isotropic material, $A = 1$. In our case, $A > 1$ indicating that both the compounds are anisotropic [22].

Spin polarized electronic and magnetic properties

Electronic charge density in terms of 3d-contour plots has been calculated to know the nature of chemical bonding in TmZn and TmCd which are shown in Fig. 3a, b. From Fig. 3a, b, it can be seen that there is no bonding charge to link the Tm and Zn (or Cd) and charge density distribution
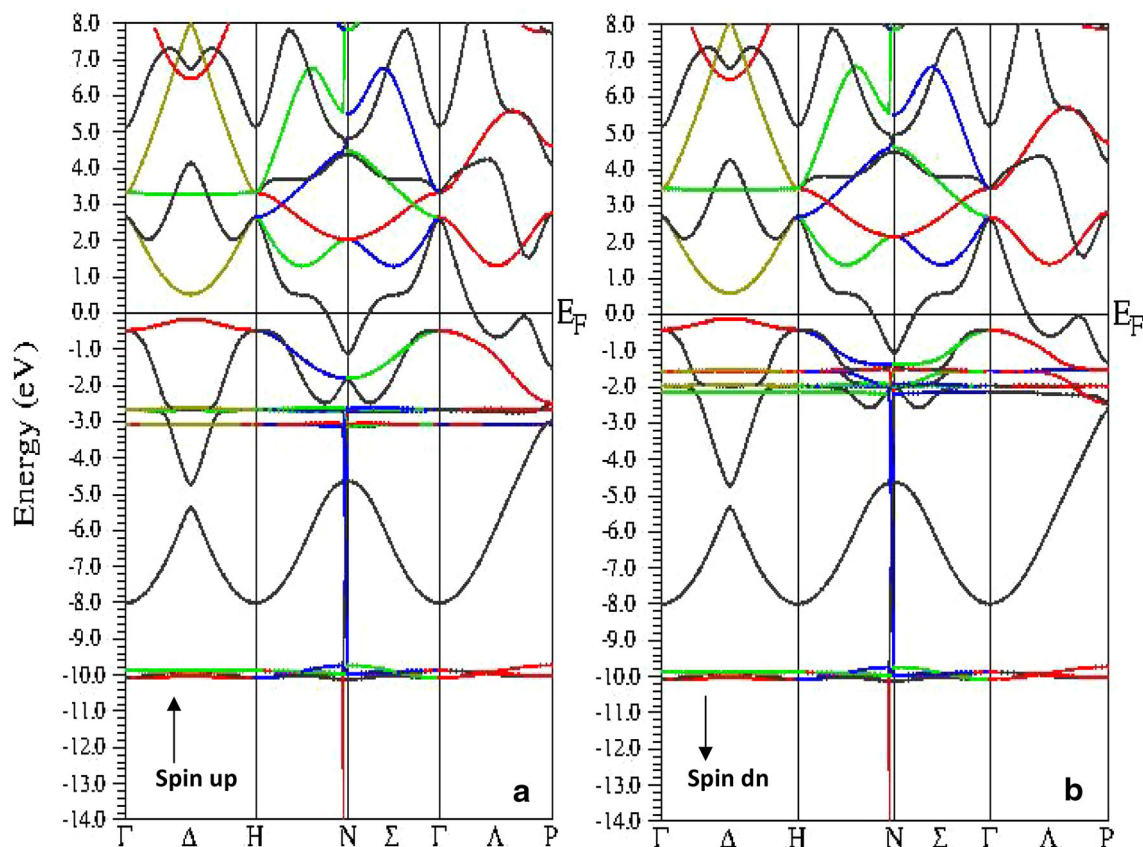
Fig. 5 a Spin polarized electron dispersion curves along high symmetry directions in the Brillouin zone for **a** TmZn_up, **b** TmCd_dn

is spherically symmetric around each atom which indicates that atoms have ionic character.

Electronic behavior of TmZn and TmCd has been shown in terms of energy bands and total, partial density of states. The calculated band structures along the high symmetry directions Γ, ΔH, N, $\sum$, Λ and P in the Brillouin zone for spin up and spin down channel have been shown in Figs. 4a, 3b for TmZn and Fig. 5a, b for TmCd. Zero value of energy gap in the both spin up and spin down band structures indicates the metallic character, whereas zero energy gap in one band structure (either spin up or spin down) is the consequence of half metallic character of the material [30]. It can be seen from these figures that most of the valence bands lie from -7.0 to 0.0 eV for TmZn and -9.0 to 0.0 eV for TmCd (where Fermi level, E_F is considered at the origin). In both the cases (spin up and spin down configuration) and for both the compounds TmZn and TmCd, the conduction bands are crossing the Fermi level (E_F) and overlapping significantly at the Fermi level (E_F) (i.e., zero energy gap), indicating typical conducting behavior. This behavior indicates that TmZn and TmCd exhibit the metallic character.

Figures 6a, f and 7a–f show the total density of states (TDOS) and partial density of states (PDOS) plots for

TmZn and TmCd, respectively. In case of TmZn, it is observed that there are three peaks in the majority spin channel below the Fermi level at around -7.0, -1.6 and -1.1 eV. The peak at around -7.0 eV is due to mainly Zn-d states (see Fig. 6e). The sharp peaks at -1.6 and -1.1 eV are due mainly due to hybridization of Zn-p and Tm-f states of majority channel (see Fig. 6d, f). For spin down, three peaks were also observed in the minority spin channel below the Fermi level at around -7.0, -0.5 eV and third one peak is just near the Fermi level. The DOS at around -7.0 eV is due to Zn-d states. DOS at around -0.5 eV is due to hybridization of Zn-p and Tm-f (see Fig. 6d, f) states and DOS near the Fermi level are due to Tm-f states.

Similarly, in case of TmCd, three peaks were observed in the majority spin channel below the Fermi level at around -9.0, -1.5 and -1.0 eV. The peak at around -9.0 eV is due to Cd-d states (see Fig. 7e). The sharp peaks at around -1.5 and -1.0 eV are mainly due to hybridization of Cd-p and Tm-f states (see Fig. 7d, f). Three peaks were also observed in the minority spin channel below the Fermi level at around -9.0, 0.8 eV and third one peak is just near the Fermi level. The sharp peak at around -9.0 eV is the result of Cd-d states while the

Fig. 6 Calculated total density of states for **a** TmZn; **b** Tm and Zn; **c** partial density of states for Tm-s, Zn-s orbital; **d** partial density of states for Tm-p, Zn-p orbital; **e** partial density of states for Tm-d, Zn-d orbital; **f** partial density of states for Tm-f orbital
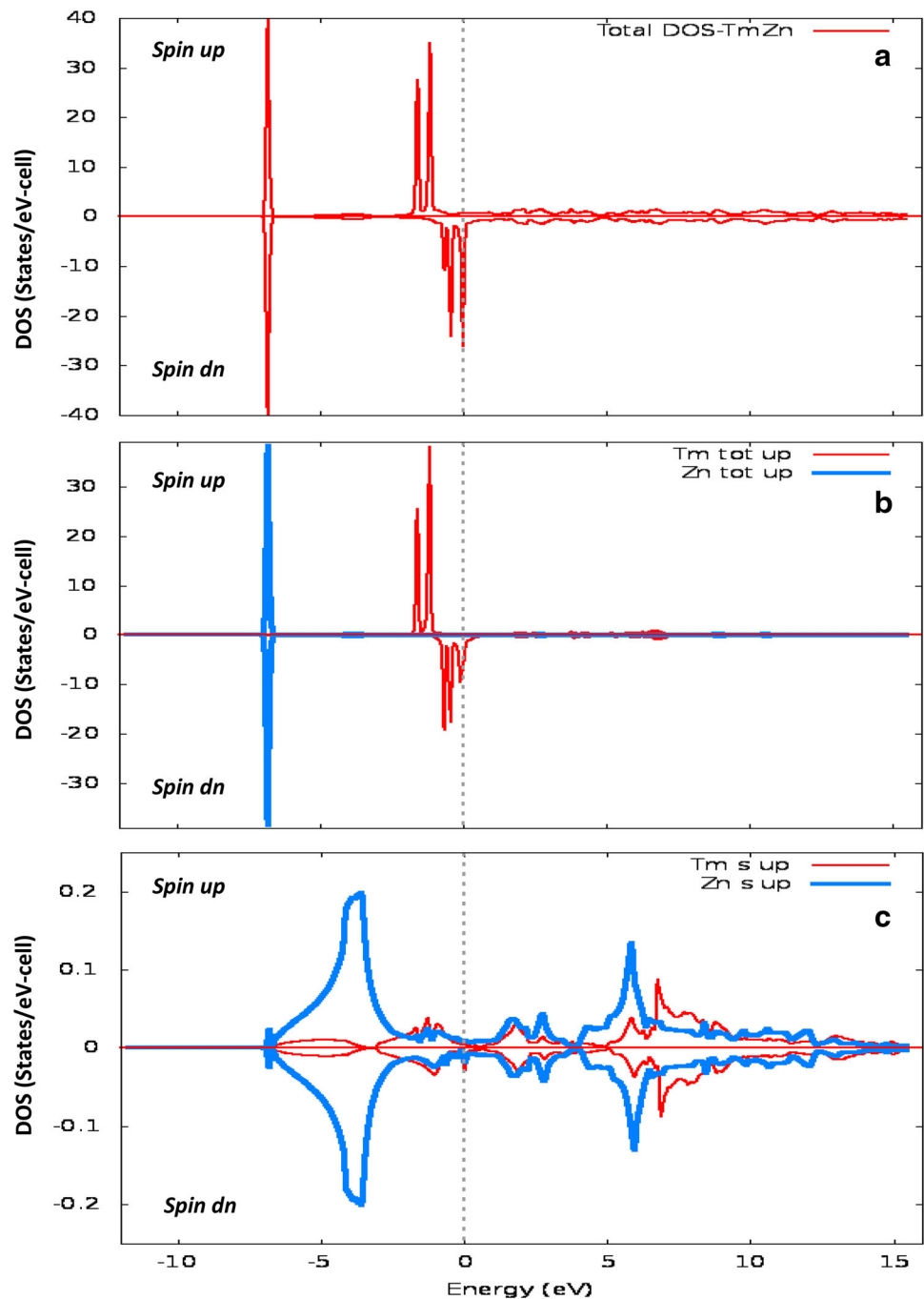

peak at around -0.8 eV is due to hybridization of Cd-p and Tm-f states (see Fig. 7d, f). The sharp peak near the Fermi level is dominated by Tm-f states. It is evident from Figs. 6a–f) and 7a–f that minority spin channel of Tm-f states are dominant near the Fermi level which is responsible for the magnetic moment. A little DOS of Zn-p (or Cd-p) are found to be empty above the Fermi level for the conduction.

The electron spin polarization at the Fermi energy (E_F) for a material can be calculated by the equation [31, 32]:

$$P = \frac{D \uparrow (E_{\mathrm{F}}) - D \downarrow (E_{\mathrm{F}})}{D \uparrow (E_{\mathrm{F}}) + D \downarrow (E_{\mathrm{F}})}. \tag{19}$$

Here, $D \uparrow (E_{\mathrm{F}})$ and $D \downarrow (E_{\mathrm{F}})$ are the density of states for majority and minority spin channel at the Fermi level, respectively. Here, $\uparrow$ and $\downarrow$ denote the spin up and spin down. The value of P identifies the type of materials, viz. zero value of P shows paramagnetic and anti-ferromagnetic character of materials even below the magnetic transition temperature. The finite value of P indicates the

Fig. 6 continued
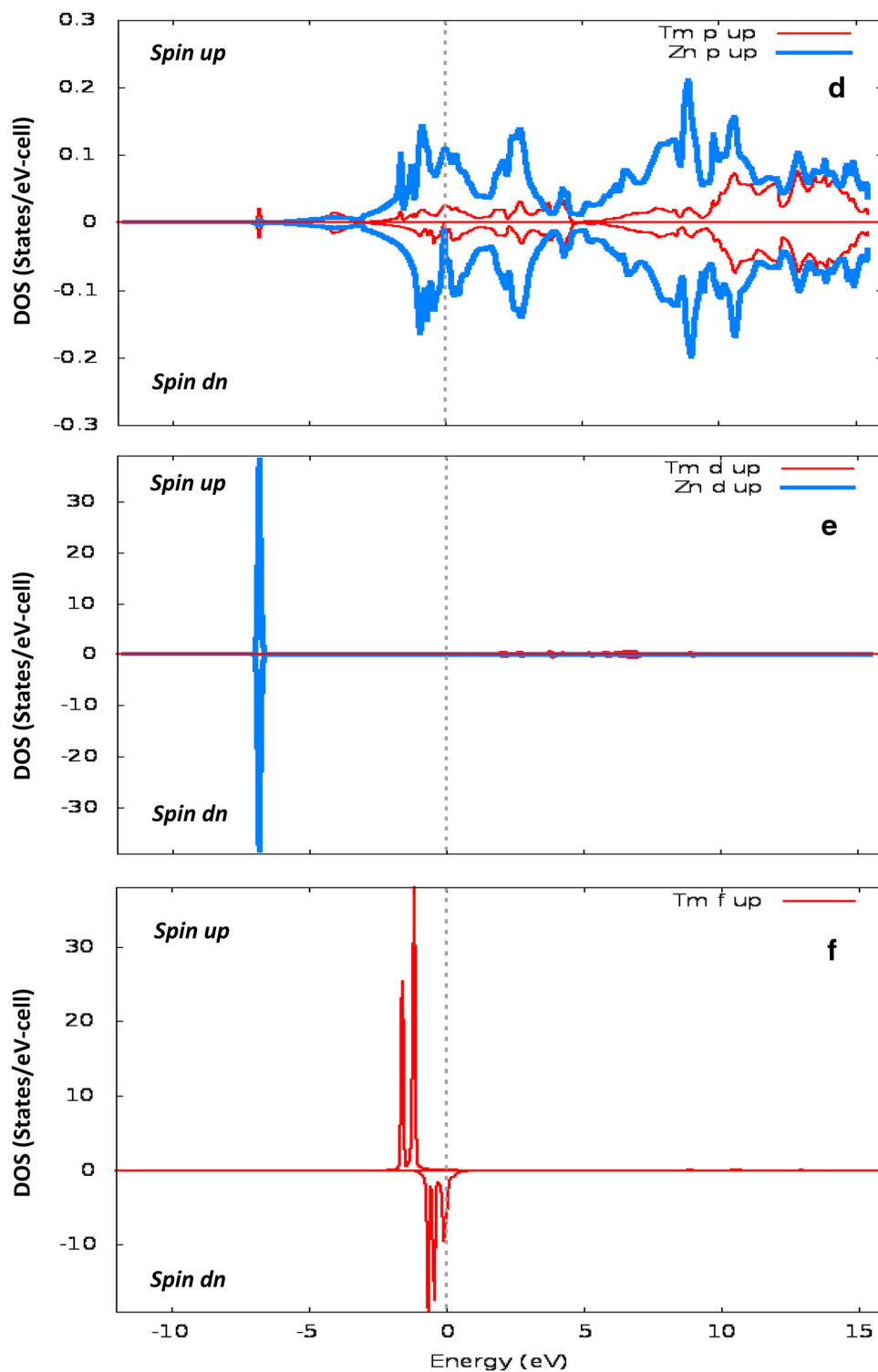
ferromagnetic material below Curie temperature [33]. Furthermore, 100 % spin polarization of electrons at Fermi level is obtained when the value of $D\uparrow(E_F)$ or $D\downarrow(E_F)$ is zero and the material is said to be fully spin polarized.

In our both the cases, neither $D\uparrow(E_F)$ nor $D\downarrow(E_F)$ vanish at the Fermi level (see Fig. 6a for TmZn and Fig. 7a

for TmCd) which gives finite value of P, implying both the compounds are typically metallic ferromagnets. The spin polarization is found to be $P \approx 92$ % for TmZn and ≈ 93 % for TmCd. High percentage values of P for both the compounds indicate that spin polarization is high in which mainly 4f-electrons of rare earth atom are

Fig. 7 Calculated total density of states for **a** TmCd; **b** Tm and Cd; **c** partial density of states for Tm-s, Cd-s orbital; **d** partial density of states for Tm-p, Cd-p orbital; **e** partial density of states for Tm-d, Cd-d orbital; **f** partial density of states for Tm-f orbital
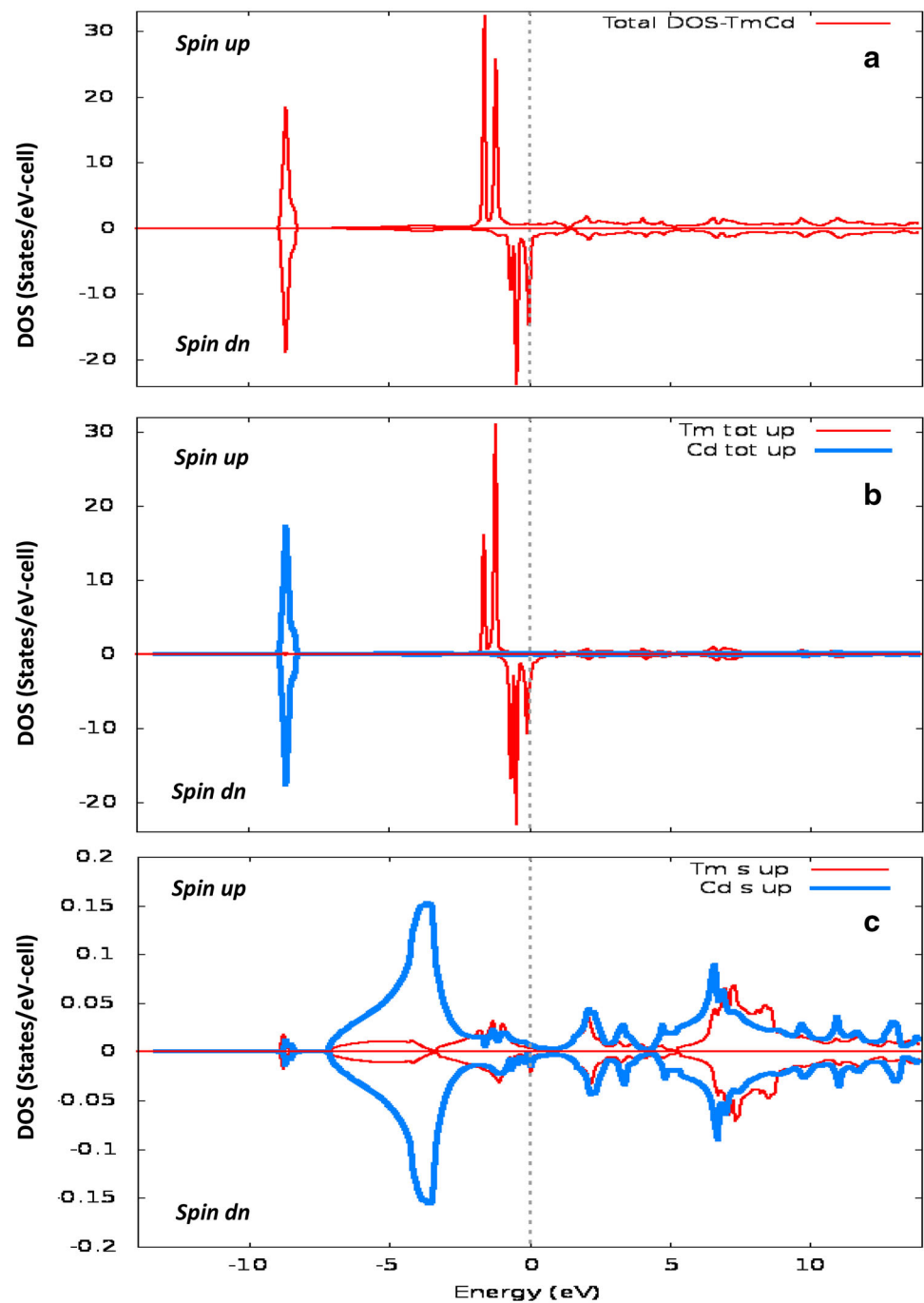
contributed mostly (see Fig. 6a, f for TmZn and Fig. 7a, f for TmCd).

In the present research paper, we have performed spin polarized electronic calculations. Therefore, it is necessary to discuss about the magnetic character of these compounds. In magnetic properties, the integer value of magnetic moment is a characteristic feature of half metallic ferromagnets, whereas fractional value of magnetic moment indicates the characteristic feature of metallic ferromagnets [30]. Calculated magnetic moments on

individual atoms and molecules are shown in Table 3. The total magnetic moment is found to be 1.2939 μ_B/formula unit for TmZn and 1.2961 μ_B/formula for TmCd. The calculated magnetic moments have been shown up to four digits after decimal. However, it does not mean that the magnetic moment is accurate up to four digits. The accuracy of magnetic moment calculated by WIEN2k package depends on the criteria of convergence and value of RMT which we are taking. These criteria have been used in the present study up to good accuracy. From Table 3, it can be
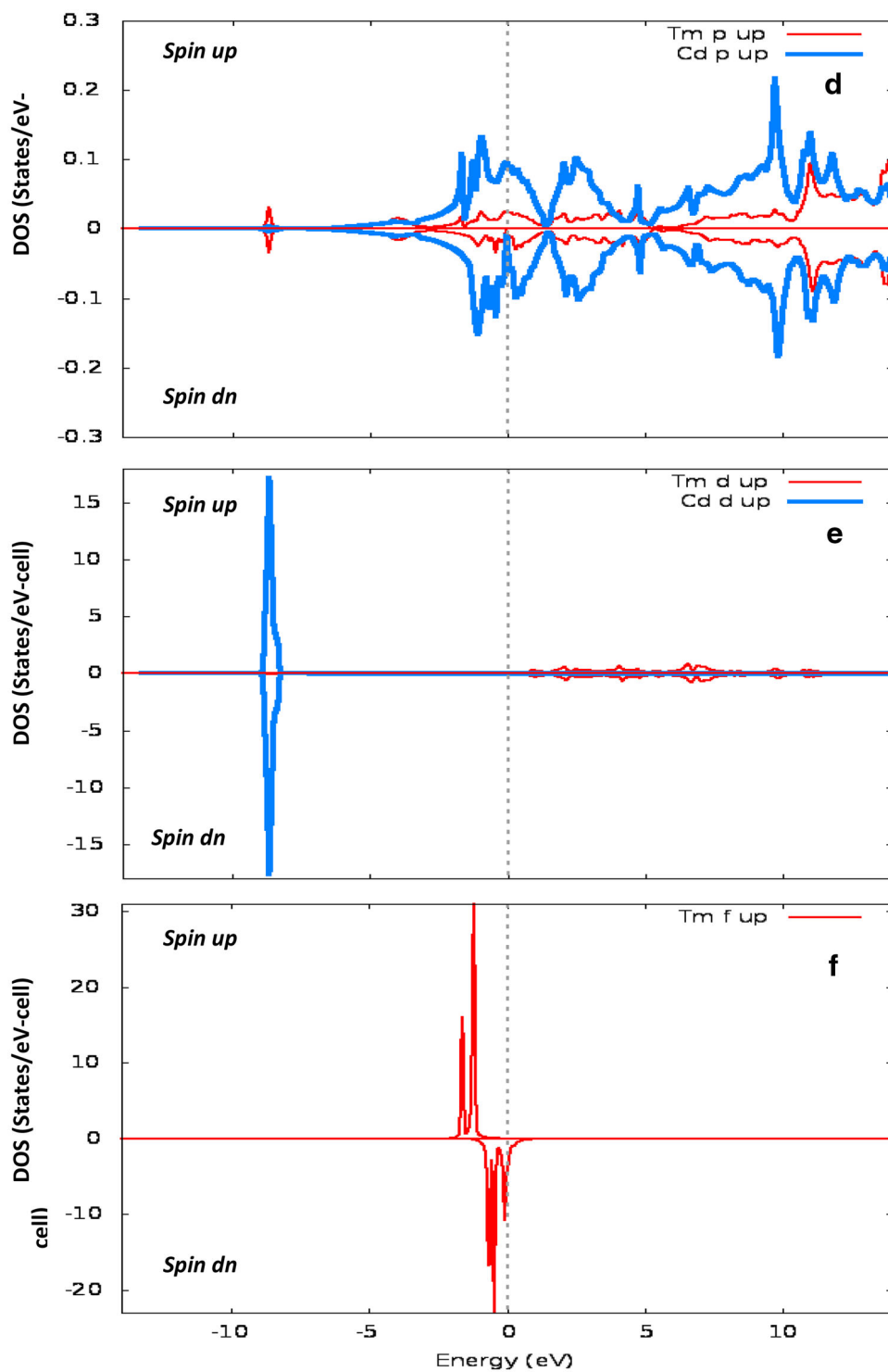
Fig. 7 continued

Table 3 Calculated spin magnetic moments (μ_B) of TmZn and TmCd

	Rare earth	Interstitial region	Zn	Cd	Total magnetic moment
TmZn	1.3133	0.0145	−0.00478	–	1.2939
TmCd	1.2996	−0.0014	–	−0.0021	1.2961
TmCu [30]	1.3626	−0.0080	−0.00815	–	1.3465

seen that total magnetic moments have fractional value which favors our results of metallic ferromagnets [30]. The total magnetic moments contain three contributions: one from the rare earth atom (Tm), Zn (or Cd) atoms and the interstitial region. Zn (or Cd) atoms and the interstitial region are found with negligible negative magnetic moments. Thus, it is concluded that net spin magnetic moment is dominated by the 4f-state electrons of the rare earth atom (Tm). The validation of calculated magnetic moment has been made by comparing present values with available theoretical values of magnetic moment for similar type of compounds [34]. Our calculated values match with good accuracy to similar type of compounds. Thus, our calculated values of magnetic moments are justified.

Conclusions

An accurate method named full-potential linearized augmented plane-wave plus local orbitals (FP-LAPW + lo) using generalized gradient approximation (GGA) has been used to study the structural, mechanical, spin polarized electronic and magnetic properties of TmZn and TmCd intermetallic compounds. The calculated lattice parameter and bulk modulus for TmZn and TmCd compounds are consistent with experimental/theoretical values. Calculated values of elastic constants and other mechanical parameters are found to be in good agreement with available theoretical/experimental values and indicate the ductile nature of TmZn and TmCd. 3d-contour plots and band structure histograms indicate the ionic character of TmZn and TmCd which is consequence of metallic character. Spin polarized electronic calculations show that studied compounds are metallic ferromagnets with high spin polarization in which mainly 4f-electrons of Tm are taking part. Magnetic behavior of TmZn and TmCd is found to be consistent with ferromagnetic nature and the total spin magnetic moment is also dominated by 4f-state electrons of the thulium.

References

1. Gschneidner Jr, K.A., Russell, A.M., Pecharsky, A.O., Zhang, Z., Lograsso, T.A., Morris, J.R., Hsu, D.K., Lo, C.H.C., Ye, Y.Y., Slager, A.J., Kesse, D.C.: New family of ductile intermetallic compounds. Nat Mater **2**, 5910 (2003)

2. Gschneidner Jr, K.A., Russell, A.M., Biner, S.B., Lo, C.H.C., Lograsso, T.A., Ye, Y., Barnard, D., Tsokol, A.O.: US Department of Energy, Basic Energy Science (2004)

3. Russell, A.M.: Ductility in intermetallic compounds. Adv. Eng. Mater. **5**, 639 (2003)

4. Russell, A.M., Zhang, Z., Lograsso, T.A., Lo, C.H.C., Pecharsky, A.O., Morris, J.R., Ye, Y.Y., Gschneidner Jr, K.A., Slager, A.J.: Mechanical properties of single crystal YAg. Acta Mater. **52**, 40333 (2004)

5. Gschneidner Jr, K.A., Russell, A.M., Biner, S.B., Harmon, B.N., Hsu, D.K., Lo, C.H.C., Lograsso, T.A., Pecharsky, A.O.: US Department of Energy, Basic Energy Science (2005)

6. Cable, J.W., Koehler, W.C., Wollan, E.O.: Magnetic order in rare-earth intermetallic compounds. Phys. Rev. **136**(1A), A240 (1964)

7. Sousa, J.B., Minto, P.P., Amado, M.M., Moreira, I.M., Braga, M.E., Morin, P.: Temperature dependence and critical behavior of the thermoelectric power in ferromagnetic TbZn compound. J. Phys. F: Met. Phys. **10**, 1809 (1980)

8. Morin, P., Williamson, S.J.: Isotropic magneto-elastic properties in thulium intermetallic compounds. Physical Review B **29**, 1425 (1984)

9. Pasha, S.K., Sundareswari, M., Rajagopalan, M.: Ab initio study of the electronic structure of some B2 intermetallic compounds. Phys. B **348**, 206 (2004)

10. Singh, R.P., Singh, R.K., Rajagopalan, M.: First-principle study on structural, elastic and electronic properties of rare-earth intermetallic compounds: TbCu and TbZn. Intermetallics **19**, 1359 (2011)

11. Shugani, M., Chouhan, S.S., Aynyas, M., Sanyal, S.P.: Ab-initio study of structural, electronic and elastic properties of ErCu. Adv. Phys. Theor. Appl. **19**, 83 (2013)

12. Singh, R.P., Singh, V.K., Singh, R.K., Rajagopalan, M.: Elastic, acoustical and electronic behaviour of the RM (R = Dy, Ho, Er; M = Cu, Zn) compounds. Am. J. Condens Matter Phys. **3**(5), 123 (2013)

13. Pagare, G., Devi, H., Chouhan, S.S.: First principles study of electronic, elastic and thermal properties of B2 -type RECd (RE = La, Ce and Pr) compounds. Int. J. Advance. Elect. Comp. Engg. **2**(8), 248 (2013)

14. Blaha, P., Schwarz, K., Madsen, G.K.H., Kvasnicka, D., Luitz, J.: WIEN2k, An Augmented Plane Wave Plus Local Orbitals Program for Calculating Crystal Properties. University of Technology, Vienna-Austria (2001)

15. Perdew, J.P., Burke, K.: Generalized gradient approximation made simple. Phys. Rev. Lett. **77**, 3865 (1996)

16. Sjostedt, E., Nordstrom, L., Singh, D.J.: An alternative way of linearizing the augmented plane wave method. Sol. Stat. Comm. **114**, 15 (2000)

17. Schwarz, K., Blaha, P., Madsen, G.K.H.: Electronic structure calculations of solids using WIEN2k package for material sciences. Comput. Phys. Comm. **147**, 71 (2002)

18. Monkhorst, H.J., Pack, J.D.: On special points for Brillouin zone integration. Phys. Rev. B **13**, 5188 (1976)

19. Buschow, K.: Rep. Prog. Phys. **42**(8), 1373 (1979). doi:10.1088/0034-4885/42/8/003

20. Charpin, T.: A Package for Calculating Elastic Tensors of Cubic Phase Using WIEN. Laboratory of geometrix F-75252 Paris, France (2001)

21. Shafaay, B.A., Hassan, F.E.H., Korek, M.: First principle investigation of mercury chalcogenides and their HgS$_x$Se$_{1-x}$ and HgS$_x$Se$_{1-x}$ ternary alloys. Comput. Mater. Sci. **83**, 107 (2014)

22. Mayer, B., Anton, H., Bott, E., Methfessel, M., Sticht, J., Schmidt, P.C.: Ab-initio calculation of the elastic constants and thermal expansion coefficients of Laves phases. Intermetallics **11**, 23 (2003)

23. Birch, F.: Finite elastic strain of cubic crystals. Phys. Rev. **71**, 809 (1947)

24. Murnaghan, F.D.: The compressibility of media under extreme pressures. Proc. Nat. Acad. Sci. USA **30**, 244 (1944)

25. Wohalfarth, E.P, Buschow, K.H.J.: Handbook of Magnetic Materials 5. Elsevier, North Holland (1990)

26. Yasui, M., Terai, T., Kakeshita, T., Hagiwara, M.: Investigation of a quadrupolar interaction in DyCu by elastic constants measurement. J. Phys. Conf. Ser. **165**, 012059 (2009)

27. Pugh, S.F.: Relations between elastic moduli and plastic properties of polycrystalline pure metals. Philos. Mag. **45**, 823 (1954)

28. Mott, P.H., Dorgan, J.R., Roland, C.M.: The bulk modulus and Poisson's ratio of incompressible materials. J. Sound and Vib. **312**, 572 (2008)

29. Yuan, P.F., Ding, Z.J.: Ab initio calculation of elastic properties of rock-salt and zinc-blend MgS under pressure. Phys. B **403**, 1996 (2008)

30. Gao, G.Y., Yao, K.L., Şaşıoğlu, E., Sandratskii, L.M., Liu, Z.L., Jiang, J.L.: Half-metallic ferromagnetism in zinc-blende CaC, SrC, and BaC from first principles. Phys. Rev. B **75**, 174442 (2007)

31. Soulen Jr, R.J., Byers, J.M., Osofsky, M.S., Nadgorny, B., Ambrose, T., Cheng, S.F., Broussard, P.R., Tanaka, C.T., Nowak, J., Moodera, J.S., Barry, A., Coey, J.M.D: Measuring the spin polarization of a metal with a superconducting point contact. Science **282**, 85 (1998)

32. Rai, D.P., Thapa, R.K.: A density functional theory study of half-metallic ferromagnets (HMFs) behavior in Co2YSb (Y = Sc, Ti). Chin. J. Phy. **51**, 812 (2013)

33. Kandpal, H.C., Fecher, G.H., Felser, C.: Calculated electronic and magnetic properties of the half-metallic transition metal based Heusler compounds. J. Phys. D Appl. Phys. **40**, 1507 (2006)

34. Chand, S., Singh, R.P., Govindan, A., Singh, S.K.: Mechanical, spin polarized electronic and magnetic properties of TmX (X = Cu, Ag): first principle study. Int. J. Mod. Phys. B **29**, 1550007 (2015)